

Discovery of Cu-Ni-Zn-Sn-Fe intermetallic compounds and S-bearing alloys in the Zhaishang gold deposit, southern Gansu Province and its geological significance

LIU JiaJun^{1,2†}, MAO GuangJian^{1,2}, MA XingHua^{1,2}, LI LiXing^{1,2}, GUO YuQian^{1,2} & LIU GuangZhi³

¹ State Key Laboratory of Geological Processes and Mineral Resources, China University of Geosciences, Beijing 100083, China;

² Key Laboratory of Lithosphere Tectonics and Lithoprobe Technology of Ministry of Education, China University of Geosciences, Beijing 100083, China

³ No.5 Gold Geological Party of Chinese Armed Police Force, Xi'an 710100, China;

Examination of ores by optical microscope and EPMA from the Zhaishang gold deposit, southern Gansu Province, has revealed an abundance of rare minerals. These include native metals, Cu-Ni-Zn-Sn-Fe polymetallic compounds and S-bearing alloys of Ni, Fe, Zn, Cu and Sn, occurring as native nickel, Zn-Cu alloy, Ni-Zn-Cu alloy, Sn-Zn-Ni-Cu alloy, Zn-Cu-Ni alloy, Zn-Fe-Cu-Sn-Ni alloy, Fe-Ni-S alloy, Sn-Fe-Ni-S alloy, Fe-Zn-Cu-Ni-S alloy, Zn-Ni-Cu-Fe-S alloy and others. Compared with the Zn-Cu alloy minerals discovered previously, these Zn-Cu minerals fall in the α or $\alpha+\beta$ portion in Zn-Cu alloy phase diagram, and the α portion has higher Cu content. Cu-Ni-Zn-Sn-Fe intermetallic compounds and S-bearing alloy minerals have not been previously reported in the literature. These rare alloys formed in a strongly reducing environment with absent oxygen and low sulfur activities.

gold deposit, native metal, polymetallic compound, S-bearing alloy, geological significance, Gansu

Ever since Fe-Ni and Fe-Ni-Co alloys were found by Melville^[1] in Oregon, the native metals and their intermetallic compounds of Fe-group elements, PGE, W-Mo group elements and sulfurized ore-forming metals have been described in lunar rock, aerolite, granite, ophiolite, kimberlite, lamproite, gabbro-diabase, quartz diorite, volcanic tuff and ore deposits of chromite, diamonds, asbestos, porphyry copper, cobalt, Cu-Ni sulfides, REE, gold, the oxidized zone of sulfides and residual talus. As examples, large quantities of native metals and alloys (Cu₂Zn, Cu₂Ni) are hosted by ophiolite in the Far-east Koryak plateau^[2-4]; PGEs and their alloys are hosted by ophiolite and chromite in Kempirsai, Kazakstan^[5]; PGEs and their alloys hosted by the ophiolite complex and alluvium in New Caledonia^[6]; abundant Fe group elements, PGEs and Cu-Zn intermetallic compounds hosted by the quartz gold deposit of Sukhol Log in Russia^[7]; the metallic films on diamond hosted by kimberlite and lamproite; and large quantities of native metals and

various of alloys such as Cu, Sn, Fe, Zn, Ni-Fe, Fe-Sn, Cu-Zn, Cu₂Zn, Cu₃Zn₂, Cu₃Sn, Cu-Zn-Pb and Pb-Sn-Cu(Au) hosted by ultramafic rock and chromite in the northern margin of Russian platform^[8]; the Cu-Zn and Cu-Sn alloys in the Sumatra placer in India^[9]; and more than 200 native metals and intermetallic compound minerals summarized by Makeev et al.^[10] in Alpine ophiolites. In China, many reports about the study of native elements and intermetallic compound were published^[11]. There have been many examples of native elements (Cu, Zn, Ni, Fe, Sn) and their intermetallic compounds from producing areas in China. They are hosted by various rocks as follows: (1) aerolite; (2)

Received October 29, 2007; accepted February 3, 2008

doi: 10.1007/s11430-008-0059-7

†Corresponding author (email: liujiajun@cugb.edu.cn)

Supported by the Major Basic Research Program of People's Republic of China (Grant No. 2006CB403500), the National Natural Science Foundation of China (Grant Nos. 40773036, 40573032 and 40434011), and the 111 Project under the Ministry of Education and the State Administration of Foreign Experts Affairs, China (Grant No. B07011)

supergene oxidation zone; (3) volcanic tuff; (4) ultra-basic-basic rocks and their deposits; (5) mid-acidic rocks and the deposits; (6) hydrothermal gold deposits; (7) SEDEX type cobalt deposit; (8) Cu-bearing carbonaceous shale and carbonate; (9) sandstone type deposit; (10) REE deposits; (11) Ag-Pb-Zn polymetallic deposits; (12) asbestos deposits; (13) alluvial deposits and artificial placers.

A large number of native metals and intermetallic compounds have been reported, but the majority are elementary substances and binary alloys. There are few reports on polymetallic compounds. Some alloys occur in legume-shape chromite grains in the Luobusha ophiolite, Tibet, such as Ni(Fe)-C-Cr, W-Cr-Co, Al-Fe-La, Fe-Si-Ti, Ag-Sn-Si, Ni-Ir-Fe, Fe-Pd-Pt and Fe-Ni-C^[12]. The S-bearing alloys are used as high-temperature materials, high temperature lubricants or surface materials in modern industrial application. Examples include Fe-S^[13], Ni-S^[14-16], C-S^[17], Si-S^[18], Fe-Ni-S^[19], Fe-Si-S^[20], Sn-S^[21], Ni-S-Co^[22], Ni-Cr-S^[23], Ni-Cr-Mo-S^[24], Ni-Fe-W-S^[25] and Ni-Fe-W-P-S^[26]. No natural S-bearing alloys have yet been reported. This article reports on Cu-Zn-Ni-Fe-Sn intermetallic compounds and S-bearing alloys.

1 Basic characteristics of the Zhaishang deposit

Located in the western part of the Min-Li metallogenetic belt, western Qinling Mountains, the Zhaishang gold deposit is a recently discovered large Carlin-type disseminated gold deposit. It occurs in the Middle Devonian and the Lower Permian, a turbidite formation composed of quartzose sandstone, siltstone, slate and limestone. The orebodies appear to be controlled by NWW-NW faults.

Based on the features of the ore-bearing protolith, ores can be grouped into two types: fine-grained sandstone type and calcareous slate type. The main sulfide minerals in the gold deposit, besides the already known pyrite, chalcopyrite, tennantite, arsenopyrite, stibnite, galena and sphalerite, include molybdenite, bournonite, guejarite, zinckenite and covellite as well as an intermetallic compound of Cu-Ni-Zn-Sn-Fe and sulfurous alloy. There are also some oxides, carbonates and sulfates. Gold mainly is present as invisible gold, but very fine-grained native gold can be occasionally seen under a microscope.

The minerals are found in a variety of textures:

mainly automorphic, hypidiomorphic, xenomorphic, framboidal, metasomatoses, pseudomorphous, microscopic girdles and cataclastic. The ores occur as vein-veinlets, breccias, disseminations, radiating, massive and drusy.

Wall rock near the mines has been altered strongly. The chief hydrothermal alteration types are the introduction of silica and calce. The intensity of hydrothermal alteration is positively correlates with the concentration of gold and associated ore minerals.

Based on the relationships of ore veins, mineral assemblages, paragenetic sequence and ore fabrics, three epochs of mineralization can be recognized as sediment-lithogenic period, hydrothermal period, and supergene oxidation period. The hydrothermal epoch can be subdivided into four stages: (1) Stage I, represented by the association of pyrite-quartz; (2) stage II, represented by the association As-bearing pyrite-arsenopyrite-pyrrhotite-quartz; (3) stage III, represented by the common association of pyrite-chalcopyrite-tetrahedrite-galena-sphalerite-stibnite-gold-calcite-quartz; (4) stage IV, represented by the association of calcite-siderite. Stages II and III are the main stages.

2 Samples collection and analysis condition

The samples of Cu-Ni-Zn-Sn-Fe intermetallic compounds and S-bearing alloys were extracted from quartzose sandstone type and calcareous slate type gold ores in the Zhaishang gold deposit. The host rocks are cut by pyrite-bearing quartz veins, disseminated by pyrite and intensely silicified and carbonatized.

The original silicified quartzose sandstone was fine-grained silty feldspar quartzose sandstone that contains abundant framboidal pyrite aggregates (Figure 1). Some have been recrystallized and formed into big spherosomes. Calcareous slate is rich in brachiopod fossils, the margins of which are replaced by pyrite. Based on the characteristics of ore type, ore mineral associations, and ore textural relations, the authors consider that these rare alloys formed during the early stages of mineralization.

Polished sections were examined with a reflecting microscope, and their minerals were analyzed by EPMA in the experimental centre of China University of Geosciences, Beijing. The EPMA instrument is a Japanese EPMA-1600 with accelerating voltage set at 15 kV, cur-

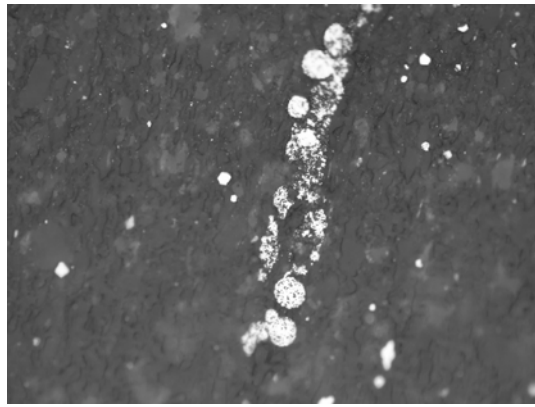


Figure 1 Abundant framboidal pyrite aggregates disseminated in quartzose sandstone type ores from Sample 06ZS-84.100× (–).

rent 20×10^{-8} A and electron beam spot diameter 0.5 μm . Standards were for Cu-chalcocopyrite, Zn-willemite, Ni-pentlandite, Sn-cassiterite, Fe-pyrite, S-barite. The dealing of the analysis data adopts ZAF-amendments.

3 Analytical results

Under the reflecting microscope, the Cu-Ni-Zn-Sn-Fe intermetallic compounds and S-bearing alloys have ir-

regular shapes which range in size from 5–15 μm (Figures 2(a)–(d)). Some of the intermetallic minerals occur as individual grains (Figure 2(a)) and some occupy fractures or the margin of pyrite (Figure 2(b)–(d)). According to the characteristics of reflection color and the results of the EPMA analyses (Table 1), these alloys can be divided into native metallic minerals, Cu-containing polymetallic compounds, Ni-containing polymetallic compounds and S-bearing alloys. They can be subdivided into different intermetallic compound based on variations in their components.

3.1 Native metallic minerals

Native nickel are identified in the ore deposit, which occurs in silicified and carbonatized sandstone-type ore as fine grains less than 5 μm . Its color is white in reflected light (Figure 2(b)). It has high reflectivity, is isotropic and is without internal reflections. The mineral is rich in Ni. Its chemical composition determined by EPMA is 91.64% Ni, 2.35% Fe, 1.70% Cu, 3.15% Sn and 1.19% Zn. A chemical formula is $\text{Ni}_{0.93}\text{Fe}_{0.03}\text{Cu}_{0.02}\text{Sn}_{0.02}\text{Zn}_{0.01}$.

Table 1 EPMA analyses of Cu-Ni-Zn-Sn-Fe intermetallic compounds and S-bearing alloys in the Zhaishang gold deposit

Serial No. ^{a)}	Sample No.	Analysis point number	Name	Element content (%)										
				Cu	Ni	Zn	Sn	Fe	Sb	Co	S	Se	As	Total
I. Native metallic mineral														
1	06ZS-84	1	native nickel	1.70	91.64	1.19	3.15	2.35				0.27		100.30
II. Cu-rich intermetallic compounds														
2	06ZS-6	q	α -Zn-Cu alloy	87.23		11.84		0.66	0.27					100.00
3	06ZS-6	r	α -Zn-Cu alloy	88.03		11.35		0.65	0.12					100.15
4	06ZS-6	s	α -Zn-Cu alloy	88.54		10.78		0.61	0.10					100.03
5	06ZS-84	a	α + β -Zn-Cu alloy	57.74	2.83	35.72		3.70						99.99
6	06ZS-84	b	Ni-Zn-Cu alloy	53.49	7.60	35.39		2.72			0.13			99.33
7	06ZS-84	h	Zn-Ni-Cu alloy	43.69	28.58	23.99		2.67			0.39			99.32
8	06ZS-84	j	Zn-Ni-Cu alloy	41.16	26.97	29.74		1.67						99.54
9	06ZS-84	p	Sn-Zn-Ni-Cu alloy	39.52	20.90	22.86	13.26	2.38			0.29			99.21
10	06ZS-84	n	Sn-Zn-Ni-Cu alloy	39.07	25.13	22.04	10.58	2.52			0.70			100.04
III. Ni-rich intermetallic compounds														
11	06ZS-84	k	Zn-Cu-Ni alloy	10.30	80.38	5.34		2.57		0.56	0.47			99.62
12	06ZS-84	m	Zn-Cu-Ni alloy	16.97	70.16	9.14	1.88	1.51			0.07			99.73
13	06ZS-84	i	Zn-Cu-Ni alloy	36.00	39.16	21.23		1.24			0.10	2.03	0.24	100.00
14	06ZS-84	o	Zn-Cu-Ni alloy	22.07	60.04	12.65	2.89	2.22			0.14			100.01
15	06ZS-84	c	Zn-Fe-Cu-Sn-Ni alloy	8.24	48.01	4.27	33.59	4.78						98.89
IV. S-bearing alloys														
16	06ZS-84	d	Fe-Ni-S alloy	0.19	65.69		2.73	14.19		0.22	15.77			98.79
17	06ZS-84	e	Sn-Fe-Ni-S alloy	5.02	57.78		14.25	12.24			11.00			100.29
18	06ZS-84	g	Fe-Zn-Cu-Ni-S alloy	32.71	31.72	16.77	0.15	8.71			9.00			99.06
19	06ZS-84	f	Zn-Ni-Cu-Fe-S alloy	21.22	19.25	11.37		22.21			25.98			100.03

a) 1, $\text{Ni}_{0.93}\text{Fe}_{0.03}\text{Cu}_{0.02}\text{Sn}_{0.02}\text{Zn}_{0.01}$; 2, $\text{Cu}_{0.88}\text{Zn}_{0.12}\text{Fe}_{0.01}$; 3, $\text{Cu}_{0.88}\text{Zn}_{0.11}\text{Fe}_{0.01}$; 4, $\text{Cu}_{0.89}\text{Zn}_{0.10}\text{Fe}_{0.01}$; 5, $\text{Cu}_{0.55}\text{Zn}_{0.35}\text{Fe}_{0.04}\text{Ni}_{0.03}$; 6, $\text{Cu}_{0.54}\text{Zn}_{0.35}\text{Ni}_{0.08}\text{Fe}_{0.03}$; 7, $\text{Cu}_{0.43}\text{Ni}_{0.30}\text{Zn}_{0.23}\text{Fe}_{0.03}$; 8, $\text{Cu}_{0.41}\text{Ni}_{0.29}\text{Zn}_{0.29}\text{Fe}_{0.02}$; 9, $\text{Cu}_{0.42}\text{Ni}_{0.24}\text{Zn}_{0.24}\text{Sn}_{0.08}\text{Fe}_{0.03}$; 10, $\text{Cu}_{0.40}\text{Ni}_{0.28}\text{Zn}_{0.22}\text{Sn}_{0.06}\text{Fe}_{0.03}\text{S}_{0.01}$; 11, $\text{Ni}_{0.82}\text{Cu}_{0.10}\text{Zn}_{0.05}\text{Fe}_{0.03}$; 12, $\text{Ni}_{0.73}\text{Cu}_{0.16}\text{Zn}_{0.09}\text{Fe}_{0.02}\text{Sn}_{0.01}$; 13, $\text{Ni}_{0.41}\text{Cu}_{0.35}\text{Zn}_{0.20}\text{Fe}_{0.01}\text{Se}_{0.02}$; 14, $\text{Ni}_{0.63}\text{Cu}_{0.21}\text{Zn}_{0.12}\text{Fe}_{0.02}\text{Sn}_{0.02}$; 15, $\text{Ni}_{0.59}\text{Sn}_{0.21}\text{Cu}_{0.09}\text{Fe}_{0.06}\text{Zn}_{0.05}$; 16, $\text{Ni}_{0.59}\text{Fe}_{0.13}\text{Sn}_{0.01}\text{S}_{0.26}$; 17, $\text{Ni}_{0.56}\text{Fe}_{0.13}\text{Sn}_{0.07}\text{Cu}_{0.04}\text{S}_{0.20}$; 18, $\text{Ni}_{0.31}\text{Cu}_{0.29}\text{Zn}_{0.15}\text{Fe}_{0.09}\text{S}_{0.16}$; 19, $\text{Fe}_{0.20}\text{Cu}_{0.16}\text{Ni}_{0.16}\text{Zn}_{0.08}\text{S}_{0.40}$.

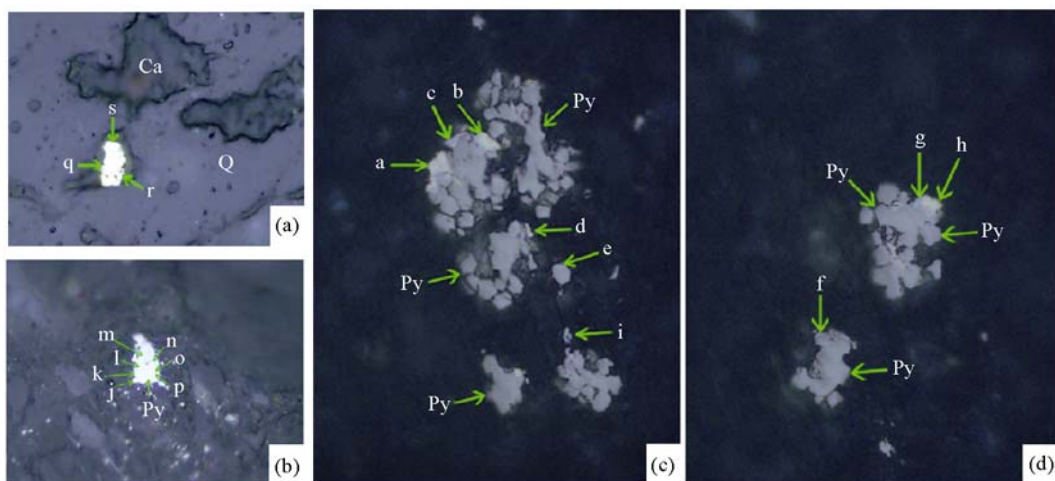


Figure 2 Photomicrographs of Cu-Ni-Zn-Sn-Fe intermetallic compounds and S-bearing alloys from Zhaishang. All photomicrographs are in reflected light. (a) Sample 06ZS-6, 100× (–); (b) Sample 06ZS-84, 100× (–); (c) and (d) Sample 06ZS-84, 400× (–). Py, pyrite; Q, quartz; Ca, calcite. a, b, c, d and others correspond to the EPMA analysis point numbers as listed in Table 1.

3.2 Cu-rich polymetallic compound

Grains 5–15 μm in size of this alloy are found in silicified and carbonatized sandstone-type and calcareous slate type of ores. Its color in reflected light is yellow-white and bright yellow (Figure 2(a)–(d)). Its reflectivity is lower than that of gold but higher than that of pyrite. It is isotropic, without internal reflection.

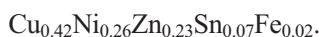
(1) α-Zn-Cu alloy mineral: The mineral contains 87.23%–88.54% Cu and 10.78%–11.84% Zn. Minor Fe and Sb are also present. The formula calculated from the average composition is $\text{Cu}_{0.88}\text{Zn}_{0.11}\text{Fe}_{0.01}$. It falls in the α portion in the Cu-Zn alloy phase diagram^[27].

(2) α+β-Zn-Cu alloy mineral: The chemical composition is Cu 57.74%, Zn 35.72%, Ni 2.83% and Fe 3.70%. This leads to a simplified formula of $\text{Cu}_{0.58}\text{Zn}_{0.35}\text{Fe}_{0.04}\text{Ni}_{0.03}$, which falls in the α+β portion in the Cu-Zn alloy phase diagram^[27].

(3) Ni-Zn-Cu alloy mineral: The chemical composition is Cu 53.49%, Zn 35.39% and Ni 7.60% with minor Fe and S present. This leads to a simplified formula of $\text{Cu}_{0.54}\text{Zn}_{0.35}\text{Ni}_{0.08}\text{Fe}_{0.03}$, which also falls in the α+β portion in the Cu-Zn alloy phase diagram^[27].

(4) Zn-Ni-Cu alloy mineral: It dominantly consists of 41.16%–43.69% Cu, 26.97%–28.58% Ni and 23.99%–29.74% Zn, with minor Fe and S. This leads to a simplified formula of $\text{Cu}_{0.42}\text{Ni}_{0.30}\text{Zn}_{0.26}\text{Fe}_{0.02}$.

(5) Sn-Zn-Ni-Cu alloy mineral: It dominantly consists of 39.07%–39.52% Cu, 20.90%–25.13% Ni, 22.04%–22.86% Zn and 10.58%–13.26% Sn, with minor Fe and S. This leads to a simplified formula of



3.3 Ni-rich polymetallic compound

This minerals occurs as grains less than 10 μm in size in fine-grained sandstone type and calcareous slate type of ores. Its color is white or silvery white in reflected light with high reflectivity similar to arsenopyrite (Figure 2(b)–(d)). It is isotropic without internal reflection.

(1) Zn-Cu-Ni alloy mineral: The chemical composition is Ni 22.07%–80.38%, Cu 10.30%–60.04%, Zn 5.34%–21.23% and minor Fe, Sn, Se, S, As. The formula calculated from the average composition is $\text{Ni}_{0.65}\text{Cu}_{0.21}\text{Zn}_{0.11}\text{Fe}_{0.02}\text{Sn}_{0.01}$.

(2) Zn-Fe-Cu-Sn-Ni alloy mineral: It mainly contains Ni (48.01%) and Sn (33.59%), with high content of Cu (8.24%), Fe (4.78%) and Zn (4.27%). Its formula is $\text{Ni}_{0.59}\text{Sn}_{0.21}\text{Cu}_{0.09}\text{Fe}_{0.06}\text{Zn}_{0.05}$.

3.4 S-bearing alloy minerals

This mineral was observed as grains less than 12 μm in size only in the fine-grained sandstone-type ores, It is white under reflected light (Figures 2(c) and (d)), isotropic and without internal reflections.

(1) Fe-Ni-S alloy mineral: its analysis is 65.69% Ni, 14.19% Fe and 15.77% S, with minor Sn (2.73%), Cu (0.19%) and Co (0.22%). This gives a formula of $\text{Ni}_{0.59}\text{Fe}_{0.13}\text{Sn}_{0.01}\text{S}_{0.26}$.

(2) Sn-Fe-Ni-S alloy mineral: It mainly consists of 57.78% Ni, 12.24% Fe, 11.00% S and 14.25% Sn, with some Cu (5.02%). This leads to a formula of $\text{Ni}_{0.56}\text{Fe}_{0.13}\text{Sn}_{0.07}\text{Cu}_{0.04}\text{S}_{0.20}$.

(3) Fe-Zn-Cu-Ni-S alloy mineral: The chemical

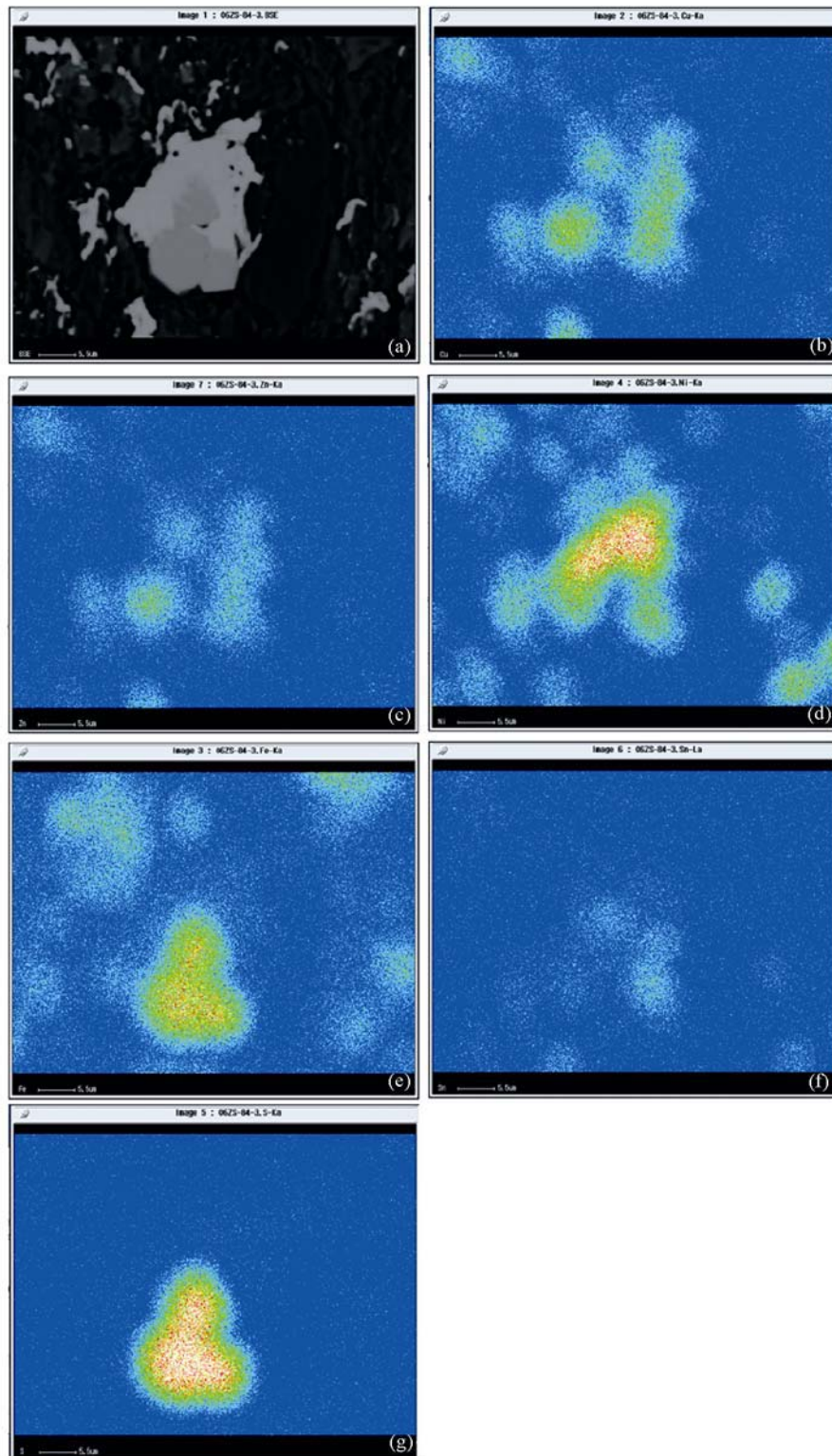


Figure 3 (a) Back-scattered electron images of the Cu-Ni-Zn-Sn-Fe intermetallic compounds and pyrite (Sample 06ZS-84, the same as in Figure 2(b)); (b)–(g) X-ray images of these polymetallic compounds and S-bearing alloys, showing relative concentration and distribution of Cu (b), Zn (c), Ni (d), Fe (e), Sn (f) and S (g).

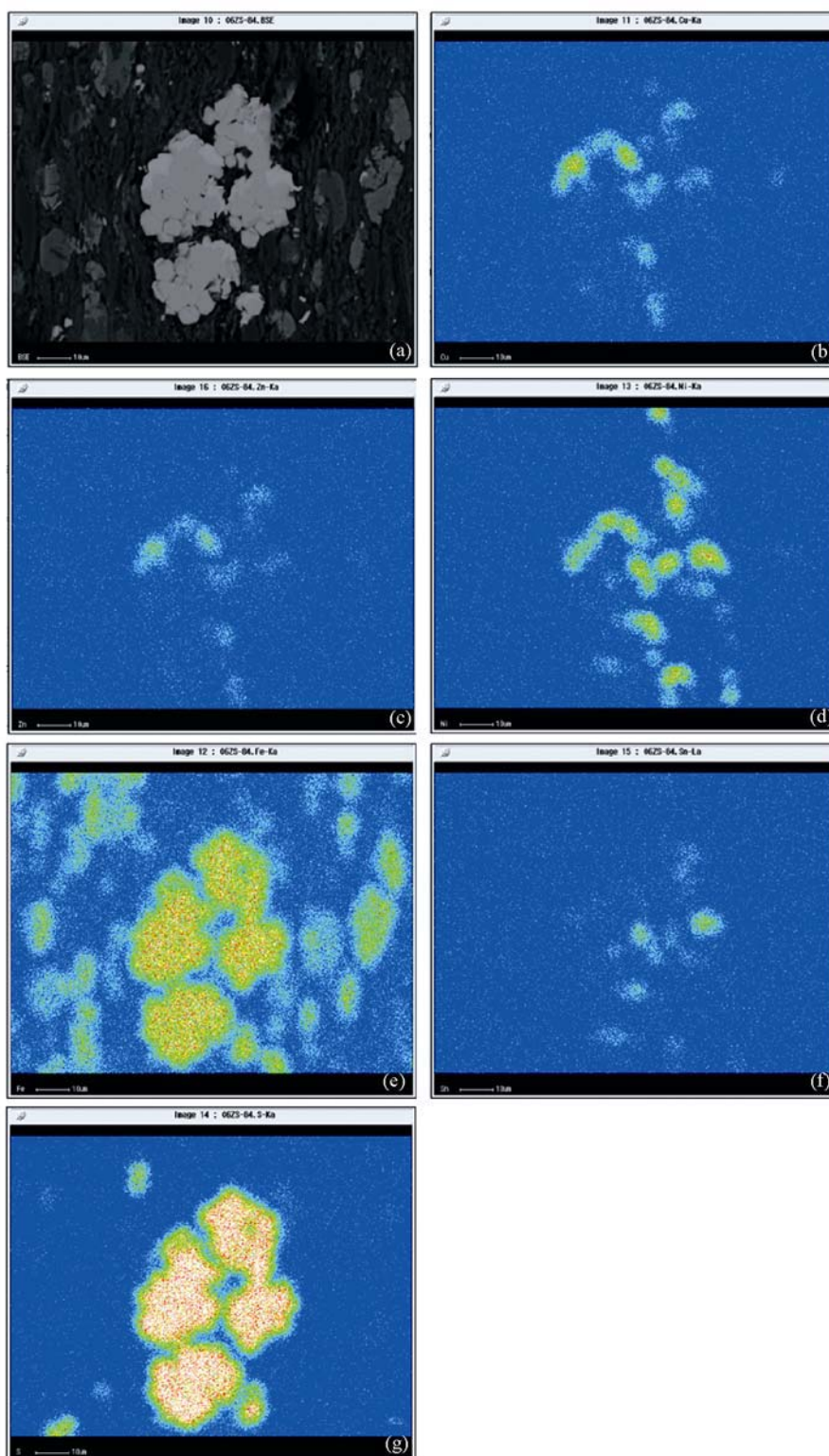


Figure 4 (a) Back-scattered electron images of the Cu-Ni-Zn-Sn-Fe intermetallic compounds, S-bearing alloys and pyrite (Sample 06ZS-84, the same as in Figure 2(c)); (b)–(g) X-ray images of these polymetallic compounds and S-bearing alloys, showing relative concentration and distribution of Cu (b), Zn (c), Ni (d), Fe (e), Sn (f) and S (g).

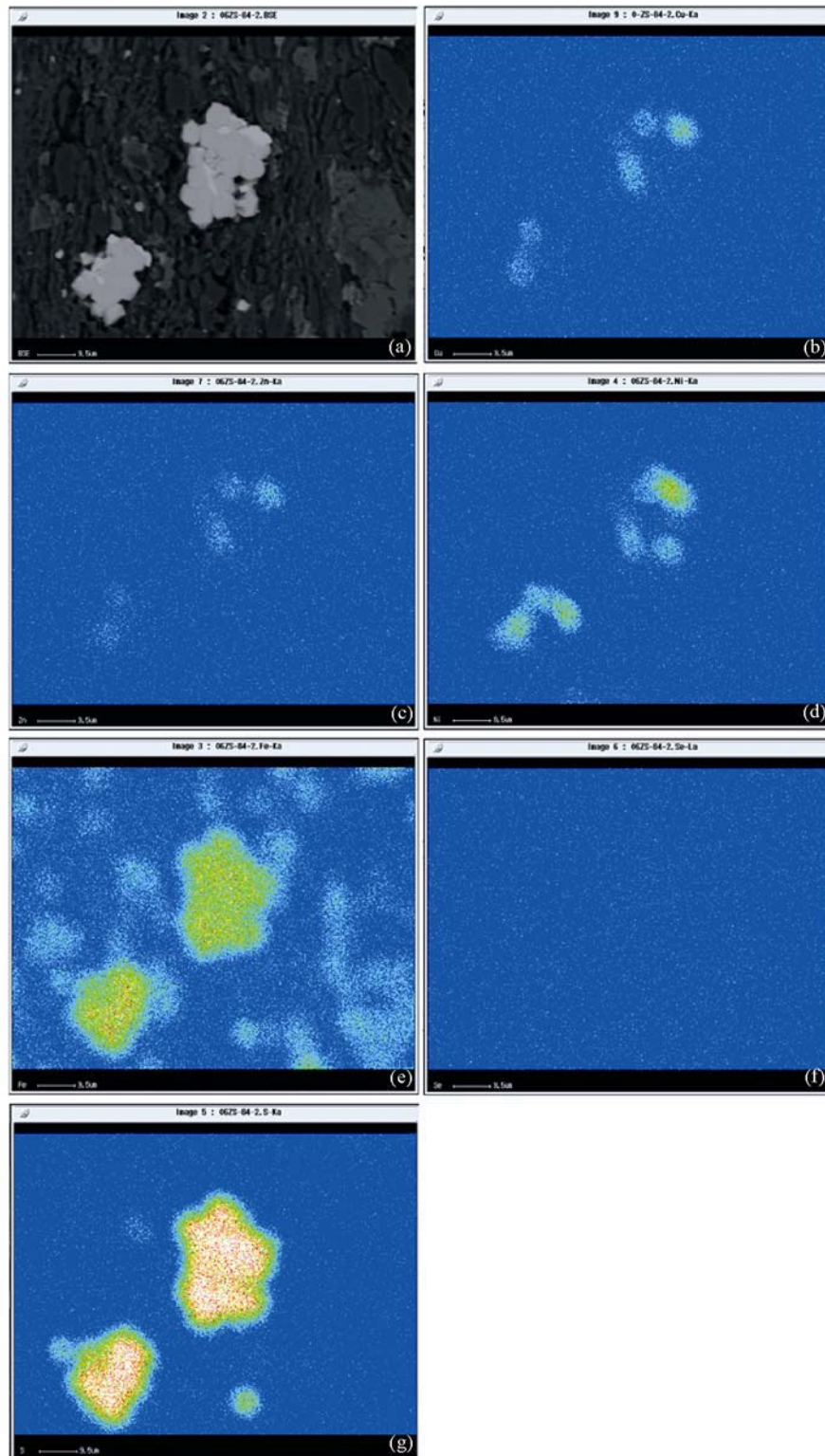


Figure 5 (a) Back-scattered electron images of the Cu-Ni-Zn-Sn-Fe intermetallic compounds and S-bearing alloys and pyrite (Sample 06ZS-84, the same as in Figure 2(d)); (b)–(g) X-ray images of these polymetallic compounds and S-bearing alloys, showing relative concentration and distribution of Cu (b), Zn (c), Ni (d), Fe (e), Sn (f) and S (g).

composition is Ni 31.72%, Cu 32.71%, Zn 16.77%, Fe 8.71% and S 9.00%, with minor Sn. Its chemical formula is $\text{Ni}_{0.31}\text{Cu}_{0.29}\text{Zn}_{0.15}\text{Fe}_{0.09}\text{S}_{0.16}$.

(4) Zn-Ni-Cu-Fe-S alloy mineral: The chemical composition is Fe 22.12%, Cu 21.22%, Ni 19.25%, Zn 11.37%, and S 25.98%, which leads to a chemical formula of $\text{Fe}_{0.20}\text{Cu}_{0.16}\text{Ni}_{0.16}\text{Zn}_{0.08}\text{S}_{0.40}$.

SEM backscatter and x-ray images of these polymetallic compounds and S-bearing alloys (Figures 3–5) show that, although there are large compositional differences in mineral grains, the elements are evenly distributed.

The S-bearing alloy is closely accompanied by pyrite. Base on the X-ray scanning images, although sulfur is evenly distributed in the minerals, the density of the distribution is apparently different, as showed in Figure 4(g), thus excluding the possibility as to the presence of any known sulfides, or the effects of the electron-scattering.

4 Discussion of genesis

Cu, Zn, Ni and Fe are located in the fourth period of periodic table, while Sn is in the fifth period. They are two different types of elements based on Goldschmidt's geochemical classification^[28]. Ni and Fe are belong to siderophile elements and Cu, Zn, Sn are chalcophile elements. Ni and Fe are metallic elements, both of which are sulphophile, and Fe is also lithophile. Therefore they can form various complex compound minerals, including native metals. Since Cu and Zn are adjacent elements in the same period of Geochemical Periodic Table, they have similar chemical characteristics, such as atomic weight (Cu 63.54, Zn 65.38), atomic radius (Cu 0.1278 nm, Zn 0.1333 nm), ionic radius (Cu^{2+} 0.072 nm, Zn^{2+} 0.074 nm) and ionic electronic potential (Cu^{2+} 2.78, Zn^{2+} 2.70). Due to their sulphophile and lithophile nature, they tend to form either sulfides or oxides if sulfur or oxygen is available. Zn is also a siderophile element. Cu and Zn usually form sulfides and sulfosalts, sometimes oxides, carbonates and silicates, and even some Cu-Zn intermetallic compounds. Sn can be lithophile, siderophile or sulphophile under different physicochemical conditions. For example, Sn occurs mainly as oxides or silicates in oxidizing conditions, forms sulfides and sulfosalts in reducing conditions where S is available, and forms intermetallic compounds with PGE

in mafic and ultramafic magma. Cu, Zn and Sn are ore-forming elements in sulfide deposits but they do not display isomorphism because they are not adjacent in the Geochemical Periodic Table^[29]. Therefore, Sn-Cu-Zn intermetallic compounds are not common and are reported in very few papers^[8].

Generally speaking, the native elements and their intermetallic compound minerals formed at the high melting temperatures under strongly reducing conditions, with O and S absent^[7]. We believe that fast upwelling and cooling of magma makes reactions between S and Cu/Zn difficult when S is either absent or present^[30]. As a result, native Cu/Zn and intermetallic minerals will quickly form instead. In the Zhaishang gold deposit, however, the Cu-Ni-Zn-Sn-Fe intermetallic compounds and S-bearing alloys occur in ultraheavy concentrates, commonly inter-grown with pyrite aggregates. They are mainly distributed on the rim of pyrite grains, or between the two grains of pyrite, which may result from exsolution. The characteristics of ore type, ore mineral associations, and ore textural relations demonstrate that the system was very low in sulfur and intermediate temperatures (280–320°C) at the beginning of mineralization (stage I) but the concentration of sulfur became very rich later (stages II–IV) allowing a lot of sulfides such as pyrite, arsenopyrite, chalcopyrite, tetrahedrite, galena, sphalerite and stibnite to form.

5 Conclusions

In the Zhaishang gold deposit, some rare minerals including native metal, the Cu-Ni-Zn-Sn-Fe intermetallic compounds and S-bearing alloys occur in ultraheavy concentrates. The characteristics of ore type, ore mineral associations, and ore textural relations demonstrate that these rare alloys formed during the early stages of mineralization. Increasing activity of sulfur results in sulfosalts and S-rich sulfide deposition. Therefore, these rare alloys formed in a strongly reducing environment with absent oxygen and low sulfur activities.

Thanks are given to Zheng Weijun, Liao Yanfu, Liu Xia and other colleagues of the Chinese People's Armed Police Force detachment of the fifth gold for their enthusiastic help with the field work. Thanks also go to Yin Jingwu, Hao Jinhua of the Experimental Center Room, China University of Geosciences (Beijing) for their great help doing the EPMA analyses. This manuscript has also benefited from the comments and critical reviews from Prof. Steven Scott at the University of Toronto in Canada.

- 1 Melville W H. Josephinite, a new nickel-iron. *Am J Sci*, 1892, 43(258): 509—515
- 2 Rudashevsky N S, Dmitrenko G G, Mochalov A G, et al. Native metals and carbides in alpine-type ultramafites of Koryak Highland. *Mineral J* (in Russian), 1987, 9(4): 71—82
- 3 Rudashevsky N S, Mochalov A G, Budko I A, et al. Pt-Ir-bearing and Ir-Pt-bearing taenite and Fe-bearing iridosmine — New mineral species. *Mineral J* (in Russian), 1988, 10 (1): 15—22
- 4 Mochalov A G, Dmitrenko G G, Zhernovskii I V, et al. A new iridium-osmium-ruthenium type (solid solutions of rare platinoids with iron) of platinoid mineralization in chrome-spinellids of alpine-type ultramafic rocks of the Koryak Highlands. *Proc Russian Mineral Soc* (in Russian), 1985, 114(5): 544—554
- 5 Melcher F, Grum W, Simon G, et al. Petrogenesis of giant chromite deposits of Kempirsai, Kazakhstan: A study of solid and fluid inclusions in chromite. *J Petrol*, 1997, 38: 1419—1458
- 6 Auge T, Maurizo T P. Stratiform and alluvial platinum mineralization in the Caledonia ophiolite complex. *Can Mineral*, 1995, 33: 1023—1045
- 7 Distler V V, Yudovskaya M A, Mitrofanov G L, et al. Geology, composition, and genesis of the Sukhoi Log noble metals deposit, Russia. *Ore Geol Rev*, 2004, 24: 7—44
- 8 Makeev A B, Bryanchaninova N I. Curve facet diamond of the north and northeast of the Russian platform. *Geosciences*, 2001, 15(2): 124—130
- 9 Bowles J F W, Cameron N R, Beddoe Stephens B, et al. Alluvial gold, platinum, osmium-iridium, copper-zinc and copper-tin alloys from Sumatra: their composition and genesis. *Appl Earth Sci*, 1984, 93: B23—B30
- 10 Makeev A B, Agafonov L V, Goncharenko A I. The relation of the chemical composition to the physical properties of chrome spinels in alpinotypic ultrabasites. *Soviet Geol Geophys*, 1984, 25(2): 125—129
- 11 Huang Y H, Yue S Q, Qin S Y, et al. The mineralogical gazetteer. In: *Nature Elements and Their Intermetallic Compounds* (in Chinese). Beijing: Geological Publishing House, 2000. 197—223, 401—421
- 12 Bai W j, Yang J S, Fang Q S, et al. Chemical compositions of alloys from podiform chromitites in the Luobusa ophiolite, Tibet. *Acta Geol Sin* (in Chinese), 2004, 78(5): 675—682
- 13 Oku M, Suzuki S, Abiko K, et al. Auger and electron energy loss spectroscopic study of surfaces of iron-sulfur alloy, Fe₇S₈ and FeS₂ cleaved in ultra high vacuum. *J Electron Spectroscopy and Related Phenomena*, 1986, 40: 227—239
- 14 Han Q, Liu K R, Chen J S, et al. A study on the electrodeposited Ni-S alloys as hydrogen evolution reaction cathodes. *Int J Hydrogen Energy*, 2003, 28: 1207—1212
- 15 Han Q, Wei X J. Electrodeposited nickel-sulfur cathode for hydrogen evolution. *J Northeast Univ (Natural Sci)* (in Chinese), 2000, 21 (5): 539—542
- 16 Si J P, Zhang J M, Huang W Q. Study on preparation of Ni-S alloys as hydrogen evolution reaction cathodes. *J Xinyang Normal Univ (Natural Sci ed.)* (in Chinese), 2006, 19(2): 210—213
- 17 Al-Dallal S, Al-Alawi S M, Aljishi S, et al. Hydrogenated amorphous carbon-sulfur alloy thin films grown from a CH₄ and H₂S gas mixture by rf glow discharge. *J Non-Crystalline Solids*, 1996, 196: 168—172
- 18 Al-Dallal S, Henari F Z, Al-Alawi S M, et al. Optical switching in hydrogenated amorphous silicon-sulfur alloy prepared by glow discharge. *J Non-Crystalline Solids*, 2004, 345-346: 302—305
- 19 Li J, Agee C B. The effect of pressure, temperature, oxygen fugacity and composition on partitioning of nickel and cobalt between liquid Fe-Ni-S alloy and liquid silicate: Implications for the earth's core formation. *Geochim Cosmochim Acta*, 2001, 65: 1821—1832
- 20 Oktay E. Effect of CaCl₂ on the desulphurization by CaO of a carbon-saturated Fe-Si-S alloy. *Annales de Chimie Science des Matériaux*, 2002, 27: 81—89
- 21 Duhalde S, Arcondo B, Sirkin H. The role of layer structure in tin oxidation kinetics. *Hyperfine Interactions*, 1991, 66: 287—294
- 22 Han Q, Liu K R, Chen J S, et al. Study of amorphous Ni-S-Co alloy used as hydrogen evolution reaction cathode in alkaline medium. *Int J Hydrogen Energy*, 2004, 29: 243—248
- 23 Que C Y, Liu J Z, Zhang G W, et al. Preparation and tribological performance of a Ni-Cr-S alloy. *Tribology* (in Chinese), 1994, 14(3): 193—204
- 24 Liu R T, Li X B, Cheng S H. Self-lubrication mechanism of Ni-Cr-Mo-S alloy. *Chin J Nonferrous Metals* (in Chinese), 2003, 13(2): 469—474
- 25 Hui W H, Zhang P, Liu J J. A study on wear resistance of new type Ni-Fe-W-S alloy brush plating layer. *Tribology* (in Chinese), 1994, 14(2): 124—133
- 26 Hui W H, Liu J J, Dennis J K. Microstructure and hardness of brush plated Ni-Fe-W-P-S alloy. *J Applied Electrochem*, 1997, 27: 105—108
- 27 Yue S Q, Wang W Y, Liu J D, et al. The research of Danba deposit. *Chin Sci Bull* (in Chinese), 1982, 27(22): 41—44
- 28 White W M. *Geochemistry*. Maryland: John-Hopkins University Press, 2007. 260—271
- 29 Liu Y J, Cao L M. *Elemental Geochemistry* (in Chinese). Beijing: Geological Publishing House, 1987. 9—25
- 30 Xie Y L, Hou Z Q, Xu J H, et al. Discovery of Cu-Zn, Cu-Sn intermetallic minerals and its significance for genesis of the Mianning-Dechang REE Metallogenic Belt, Sichuan Province, China. *Sci China Ser D-Earth Sci*, 2006, 49(6): 597—603